Spectroscopic characterization of a neon surface-wave sustained (2.45 GHz) discharge at atmospheric pressure

A. Sáinz and M.C. García*

Grupo de Espectroscopía de Plasmas, Universidad de Córdoba Edifico C-2, Campus de Rabanales, Córdoba (Spain)

Abstract

In this paper a spectroscopic study of a microwave (2.45 GHz) neon surface-wave sustained discharge (SWD) at atmospheric pressure in a quartz tube has been carried out in order to determine the plasma characteristic parameters (e.g electron temperature and density, gas temperature, absorbed power per electron) and also to identify possible deviations from the thermodynamic equilibrium for this kind of microwave discharge. The results have been compared to experiments in the literature for other noble gas (helium and argon) SWDs generated under similar experimental conditions. Intermediate values between those of argon and helium plasmas were obtained for characteristic neon plasma parameters (temperatures and electron density). An important departure from the Saha equilibrium was exhibited by neon SWDs.

Keywords: microwave discharge; optical emission spectroscopy; atmospheric pressure; neon.

**Corresponding author. Tel. 34 957 212068 FAX. 34 957 212068*

e-mail address: fa1gamam@uco.es

1. Introduction

There has been a growing interest in the study of microwave induced plasmas (MIPs) in recent years due to the increased use of this kind of discharge in a number of scientific and technological fields. Nowadays, MIPs are being used in analytical chemistry, in spectroscopy, in the sterilization of medical instruments, for gas detoxification, in surface processing [1-4], etc. A large set of MIPs has been developed in the last two decades [1, 5-17]. Among them, surface-wave sustained discharges (SWDs) in dielectric tubes [1] are especially interesting because of their unique features such as high flexibility, ease of handling and their ability to be generated under broad ranges of experimental conditions (pressure, frequency, type of gas). Moreover, the length of SWDs can be easily changed by applying different microwave powers. In recent years a significant number of theoretical and experimental works have been conducted on the behavior of this type of plasma under atmospheric pressure [18-24]. However, the most of them focus their attention on helium and argon plasmas and there have been few experimental studies on the characterization of surface-wave neon discharges sustained at this pressure condition. As far as we know, only the works of Kabouzi *et al.* [24] and Kabouzi and Moisan [25], on the study of the contraction and filamentation of (argon, helium, neon, nitrogen) SWDs at atmospheric pressure can be found in the literature.

In the field of analytical spectrometry, helium is advantageously used to generate plasmas intended for applications to detect elements with a high ionization potential, such as non-metals. This is due to the fact that metastable and excited states of helium plasmas have a higher excitation energy (≥ 19.73 eV) than that of argon plasmas (≥ 11.62 eV). However, the use of high microwave power (≈ 1-2 kW) is necessary to create and maintain helium SWDs at atmospheric pressure [24] and a short column of a

typical 10 cm in length is achieved at 2kW. On the contrary, microwave argon SWDs can be generated with only a few watts (~ 25 W) [18-21] and longer columns can be generated (40 cm at 500 W). The metastable and excited levels of a neon discharge have excitation energy over 16.67 eV and it is possible to maintain stable neon SWDs of about 7 cm by using a microwave power of 200 W. So, it is of great interest to research the possibility of using neon as an alternative to argon and helium gases to generate microwave discharges and study the possible advantages of the use of this kind of plasma in some applications.

In this work, a thorough experimental analysis of a microwave (2.45 GHz) neon surface-wave sustained discharge maintained at atmospheric pressure has been carried out in order to determine the plasma characteristic parameters (e.g electron temperature and density, gas temperature, absorbed power per electron), and to identify its possible deviations from the state of thermodynamic equilibrium.

Densities of the excited states and the physical quantities that characterize the plasma have been determined by using Emission Spectroscopy techniques (non invasive techniques). The experimental results obtained in this work were compared with theoretical ones obtained by Nowakowska *et al*. [26] from a two temperature fluid model for a neon microwave discharge at atmospheric pressure, resulting in a good agreement.

This paper has been organized as follows. The next section briefly describes the possible deviations from the thermodynamic equilibrium state for laboratory plasmas while Section 3 indicates the diagnosis techniques employed to determine characteristic plasma magnitudes. Section 4 describes the experimental setup used to generate and diagnose the discharge. Finally, Section 5 presents and discusses the experimental

results obtained in this work and Section 6 highlights the most interesting conclusions to be drawn.

2. Characterizing the departure from thermodynamic equilibrium

It is well known that local thermodynamic equilibrium (LTE) is the closest possible state to complete thermodynamic equilibrium (TE) in laboratory plasmas. When the plasma is in LTE, all plasma species are characterized by the same temperature, so it is plausible to define a "plasma temperature". A deviation from LTE occurs when the kinetic energy transferred between electrons and heavy particles is no longer sufficient to distribute energy evenly among them because of the large mass difference involved. Nonetheless, provided that the interaction among particles of a given type is strong enough, these particles obey a Maxwellian energy distribution, viz. one for electrons, characterized by the electron temperature (T_e), and the other for heavy particles characterized by the gas temperature (T_{gas}). These discharges are known as two-temperature plasmas (*2T* plasmas) [27-28]. In a *2T* plasma, if the electron density is high enough to ensure that the electrons are solely responsible for the plasma excitation/de-excitation mechanisms, a situation close to LTE can appear and the Atomic State Distribution Function (ASDF) is described by the Saha-Boltzmann distribution, given by [27]

$$n^S(p) = \frac{h^3}{(2\pi m_e k T_e)^{3/2}} \frac{g_p n_e^2}{2 g_+} \exp\left(\frac{E_{ip}}{k T_e}\right) \qquad (1)$$

where $n^S(p)$ is the Saha density of excited atoms in level with an effective quantum number p and g_p its degeneracy, n_e is the electron density, T_e the electron temperature,

and E_{ip} the ionization potential of the atom in level p. This number is defined as $p \equiv \zeta (E_H / E_{ip})^{1/2}$, ζ being the core charge of the atom and E_H the ionization potential of hydrogen. In this case, the production and destruction of free electrons is governed by the so called *Saha balance*

$$A_p + e^- \leftrightarrow A^+ + e^- + e^- \qquad (2)$$

that is verified for all levels of the atomic system. The plasma is said to be in *Local Saha Equilibrium* (LSE).

In LSE, the *Boltzmann balance* describing the exchange of internal atom energy with the kinetic energy of free electrons

$$A_p + e^- \leftrightarrow A_q + e^- \qquad (3)$$

is also in equilibrium for each pair of levels.

However, occasionally electrons cannot control the full ASDF, but only part of it. In microwave discharges, a partial Local Saha Equilibrium (pLSE) is frequently found [18,19,21,29,30]. In this case, the atomic energy system splits into two regions, one at the top where the Saha balances (2) are conserved and the level populations are given by (1), and the other at the bottom, where elementary balances are controlled by improper balances [27-28] and the levels are underpopulated (pLSE recombining) or overpopulated (pLSE ionizing) with respect to the Saha equilibrium. These deviations might result from the existence of gradients in the plasma leading to diffusive processes that alter the balance (2) [31].

In order to readily characterize the type (ionizing versus recombining) and the degree of departure from LSE of an atomic system, it has become standard to use the $b(p)$ parameter defined as

$$b(p) = \frac{n(p)}{n^S(p)} \equiv \frac{\eta(p)}{\eta^S(p)} \qquad (4)$$

where the density $n(p)$ of excited atoms in level p is normalized to the Saha equilibrium density $n^S(p)$. The third member of Eq. (4) is written in terms of the density per statistical weight $g(p)$ [$\eta(p) \equiv n(p)/g(p)$], which is the number density of a state with excitation energy E_p. Thus, in this formalism, provided with $b(p)$ the energy system's excited levels, one can distinguish between *ionizing* and *recombining* plasmas depending on whether $b(p) > 1$ or $b(p) < 1$ for lower lying levels, respectively; the degree of equilibrium is close to (or far from) LTE when $b(p)$ for the lower levels is close to unity (or far from it). A more detailed discussion on pLSE and the physical processes that determine it can be found in Refs. 18-23, 27-28 and 32-33.

So, in studying the type of equilibrium prevailing in laboratory plasma, the atomic-state distribution function should be known as accurately as possible. On the other hand, the ASDF is the result of all of the elementary processes occurring in the plasma and so possesses valuable information about microscopic processes. In this paper the ASDF has been plotted in the so-called *Boltzmann plot*, which reflects the dependence of the population of the atomic states on their respective excitation energies.

3. Diagnosis methods

Characteristic quantities of the plasma were determined by using Emission Spectroscopy techniques. Atomic Emission Spectroscopy (AES) techniques were used to measure the electron density, electron temperature and population density of excited states, and Molecular Emission Spectroscopy techniques to estimate the gas temperature. A brief comment on the procedure followed in each case is presented below.

3.1. Electron density

The *electron density* (n_e) was determined from the Stark broadening of the H_β Balmer series line (486.13 nm) of the hydrogen atomic system. Hydrogen atoms were present in the discharge because of impurities in the carrier gas (neon of 99.99% purity). The Stark broadening of the H_β line is one of the most common tools for the diagnosis of plasma electron density because this broadening is slightly dependent on electron temperature as well as on its profile of phenomena, such as *ion dynamics* [34]. Moreover, the tables and expressions available in the literature [34-35] relating the Stark profile of the H_β line to electron density are very accurate. In the present work, the Gigosos *et al.* [36] expression was used to calculate n_e from $\Delta\lambda_S(H_\beta)$ (full width at half-maximum FWHM of the Stark unfolded line)

$$\Delta\lambda_s(H_\beta) = 4.800nm \times \left(\frac{n_e}{10^{23}m^{-3}}\right)^{0.68116} \quad (5)$$

with n_e in m^{-3} and the $\Delta\lambda_S$ in nm. The calculations cover the n_e-range of between 10^{20} and 10^{25} m^{-3} and of T_e between 1 000 and 17 500 K.

The magnitude of the experimental Stark broadening of the H_β line was calculated by numerically fitting its experimental profile to a Voigt function (a result of the convolution of a Gaussian function with a Lorentzian function). Under the experimental conditions of the plasma studied, the Lorentzian part of the H_β profile could be largely ascribed to the Stark effect [35].

The error in the data, obtained from the standard deviation of n_e upon repeating the H_β recording 6 times at a given plasma position was around 10%.

3.2. Plasma temperatures

The *gas temperature* (T_{gas}) was considered as being equal to the rotational temperature T_{rot} obtained from the rotational spectrum for the Q_1 branch of the (0-0) of the OH radical between 306 and 311 nm, which came from the dissociation of water traces present in the plasma gas. The highly favorable energy exchange between heavy particles in the plasma and the internal roto-vibrational states of these molecular species via collisions allowed this assumption to be made [37]. Likewise, Ricard *et al.* [9] have utilized N_2^+, N_2, *CN*, and OH as thermometric species in an argon microwave discharge at atmospheric pressure. They found that the value of T_{gas} obtained from N_2^+, N_2, and *CN* agreed, within experimental error, and the OH band was a reliable thermometer variable for $T_{gas} \leq 1\ 800$ K. In our case, very weak bands for N_2^+, N_2, and *CN* were detected, so the OH band was used for T_{gas} determination.

The value of T_{gas} was taken from the slope of the plot of $\log(I\lambda/A)$ as a function of transition upper state energy, I being the maximum value of the line intensity and A the corresponding transition probability (Table 1). The standard deviation on T_{gas} was under 15% upon repeating the recording six times.

On the other hand, the *electron temperature* (T_e) was estimated from the line-to-continuum method [38-39]. The use of the Boltzmann-plot method employed in argon SWDs [18, 21] to determine the electron temperature from the excitation temperature was discarded because this is an unreliable method in plasmas far away from LTE [40] like the neon SWDs studied in the present work (see *Section 5.4*).

The line-to-continuum method is based on the measurement of the ratio of the relative intensity of an isolated line (I) and its neighboring continuum ε_c, which is related to T_e through the expression

$$\frac{I}{\varepsilon_c} = \left(\frac{3\sqrt{3}h^4}{4e^6} \right) \left(\frac{c^3 \varepsilon_0^3}{k} \right) \frac{A_{pq} g_p}{Z^+} \frac{\lambda}{T_e \xi} \exp\left(\frac{E_{ion}}{kT_e} - \frac{E_p}{kT_{exc}} \right) \qquad (6)$$

where ξ is the free-bound Gaunt factor, Z^+ the partition function of singly ionized atoms, E_{ion} the ionization potential of neon, A_{pq} the coefficient for spontaneous emission from level p to level q, λ the wavelength of the corresponding transition, g_p the statistical weight of the level p, E_p the excitation energy of the level p, and T_{exc} the excitation temperature that relates the population of level p to that of the ground state [41]. This calculation was done for three lines of neon: 692. 95, 717.39 and 724.52 nm. The values of electron temperature estimated in this way were consistent with those obtained from electron-atom collision frequency, taking advantage of the relationship existing between the two parameters, as will later be seen in Section 5.1.

3.3. Population of the metastable and resonant states

The population of Ne($^3P_0$) and Ne($^3P_1$) states was obtained using *self-absorption techniques* [42-44]. The ratio of the total intensities of two partially self-absorbed lines emitted by the discharge (both ending at the same level whose population one aim to determine) was measured.

Assuming that the medium (plasma) is homogeneous in the observation direction, the emissivity, $J(\upsilon)$, and the absorption coefficient, $k(\upsilon)$, do not depend on the spatial coordinates and it is presumed that they have the same spectral profile. The total transmitted intensity at the end of the medium, I, can be expressed as [42]

$$I / I_0 = W / Sl \qquad (7)$$

where I_0 is the total transmitted intensity in the absence of absorbing atoms and l is the length of the medium in the observation direction. In the expression (7), W is the equivalent width of the line given by

$$W = \int \left[1 - \exp(-k(\upsilon) \cdot l)\right] d\upsilon \qquad (8)$$

and S is the strength of the line defined as

$$S = \int k(\upsilon) d\upsilon = \frac{\pi e^2}{mc} n_p f_{pq} \qquad (9)$$

f_{pq} being the oscillator strength and n_p the absorbing atoms concentration.

For a Voigt profile, the absorption coefficient has the expression:

$$k(\upsilon) = k_0 \frac{a}{\pi} \int \frac{\exp(-y^2)}{a^2 + (\omega - y)^2} dy \qquad (10)$$

where

$$\omega = 2(\upsilon - \upsilon_0)\sqrt{\ln 2} / \Delta\upsilon_D \qquad (11)$$

and a is the so-called *damping parameter*

$$a = \Delta\upsilon_L \sqrt{\ln 2} / \Delta\upsilon_D \qquad (12)$$

The a parameter gives the ratio between the Lorentzian and Doppler widths at half height of the line, $\Delta\upsilon_L$ and $\Delta\upsilon_D$, respectively. This parameter characterizes the profile shape of the lines and depends on the state of the plasma, e.g. on gas temperature and electron density.

In this case (Voigt profile), the ratio between the line intensities can be written as:

$$I / I_0 = 2\left(\frac{\ln 2}{\pi}\right)^{1/2} \left(\frac{1}{k_0 l}\right) \left(\frac{W(k_0 l, a)}{\Delta\upsilon_D}\right) \qquad (13)$$

with $\Delta\upsilon_D$ done by:

$$\Delta\upsilon_D = 2\sqrt{2R\ln 2}\,\frac{\upsilon_0}{c}\sqrt{\frac{T_{gas}}{M}} \qquad (14)$$

and k_0 expressed as:

$$k_0 = \frac{2e^2}{mc}\sqrt{\pi \ln 2}\,\frac{n_q f_{pq}}{\Delta\upsilon_D} \qquad (15)$$

From these expressions, the metastable and resonant population of the argon can be obtained.

The method employs two lines ending at the same level (for which one wishes to determine the population): line (1), for which the oscillator strength is highest, will be more strongly absorbed than line (2). From the total intensities emitted by these lines in the absence of absorption, I_{01} and I_{02}, and the total self-absorbed intensities, I_1 and I_2, the ratio of these amounts (which depends on the population of the absorbing level) can be written as follows

$$r = \frac{I_1}{I_2} \Big/ \frac{I_{01}}{I_{02}} = \frac{k_{02}}{k_{01}} \frac{W(k_{01}l, a_1)}{W(k_{02}l, a_2)} \frac{\Delta\upsilon_{D2}}{\Delta\upsilon_{D1}} = r\left(k_{01}l, \frac{k_{01}}{k_{02}}, a_1, a_2\right) \qquad (16)$$

where

$$\frac{k_{02}}{k_{01}} = \frac{f_2\upsilon_1}{f_1\upsilon_2} \qquad (17)$$

is constant for a chosen pair of lines, υ_1 and υ_2 being the experimental frequencies at the centers of lines (1) and (2), respectively. The values of a_1 and a_2 are obtained from the Doppler and the Lorentzian broadenings of the spectral lines.

The ratio I_{01}/I_{02} can be measured by measuring the intensities of lines (1) and (2) along a plasma direction small enough in length, in which the absorption can be neglected. On the other hand, I_1/I_2 can be determined by measuring the line intensities along a longer direction. In the plasma column studied in this work, whose diameter (2.5mm) is much smaller than its length (typically l = 65 mm), I_{01}/I_{02} and I_1/I_2 were *side-on* and *end-on* measured, respectively.

By using the values of r determined experimentally and the relationship (16), the value of the coefficient k_{01} of the most self-absorbed line was obtained. Finally, from equation (15) it is possible to calculate the metastable (and resonant) atom concentrations whose error was estimated (from the standard deviation upon repeating

the recordings six times) to be around 20%. A more detailed description of this method can be found in Refs. 43 and 44.

3.4. Population density of the NeI excited states

The absolute populations of the different atomic levels n_p of neon system were determined from calibrated measurements of the intensity I of the spectral lines emitted by the plasma [45], corresponding to atomic transitions starting at each specific level, using the following expression

$$I = \frac{hc}{4\pi}\frac{A_{pq}}{\lambda}n_p \qquad (18)$$

where A_{pq} is the coefficient for spontaneous emission from level p to q and λ the wavelength of the corresponding transition. The neon atomic lines detected in this work and their spectroscopic features are shown in Table 2 [46]. The error in the n_p measurements of about 20 % was mainly determined by the accuracy of the absolute intensity calibration.

On the other hand, in the discharges studied, the ground state population of the NeI system was much greater than that of any other species present in the plasma. Thus, the population of the ground state, n_1, could be determined from the ideal gas equation

$$p = n_1 kT_{gas} \qquad (19)$$

where the pressure (p) was 1 atm, and T_{gas} was the previously measured gas temperature.

4. Experimental set-up

The neon surface-wave sustained plasmas studied were generated in a quartz tube, by using a *surfaguide* launcher device [1], which allowed microwave (f = 2.45 GHz) energy to be coupled to the discharge (see Fig. 1). This device launched surface waves along the discharge tube direction in two ways, creating and sustaining a plasma column that extended to both sides of it (Fig. 1). The part of the plasma in which the direction for both surface wave propagation and flow gas is the same is called the *downstream column*. The other part of the plasma is the so-called *upstream column*. Thus, the full length of the plasma column results from the addition of the lengths of the downstream column, the upstream column and that corresponding to the launcher *gap* (of 1 cm). The injected microwave power (P_i) was 400 W; and the full plasma length was about 14 cm. This plasma length was enough to perform the axial study of the column. The movable plunger and pistons permitted the impedance matching so that the best energy coupling could be achieved, making the power reflected back to the generator (P_r) negligible (< 5%). In this way, the power absorbed by the discharge (P_{abs}) is considered equal to the difference between P_i and P_r.

High frequency plasmas sustained with either rf or microwave fields at high enough pressures (typically higher than 10 Torr in rare gases) are radially contracted [24]. An effect related to contraction phenomenon is the so called plasma *filamentation*: at high enough electron densities the plasma column splits into two or several filaments of smaller diameters, the discharge often being unstable in this situation. In the case of

neon SWDs maintained at atmospheric pressure and microwave frequency of 2.45 GHz, no contraction or filaments were observed using tubes with diameters of less than 6 mm, contrarily to what occurs in the argon discharges which show radial contraction and filaments in tubes with 3 mm inner diameter [24]. The discharges were created in tubes with an inner diameter that were small enough to ensure that the plasma was stable and well centered at the axis. Thus, the neon plasma in the present work was created within a quartz capillary tube of 2.5-mm inner diameter in order to prevent its contraction and filamentation.

The support gas of the discharge was 99.99% pure neon, flowing at 0.5 l/min and coming out into the room through the open end of the discharge tube. The study performed was restricted to the analysis of the downstream column.

Figure 1 also depicts the optical detection assembly and the data acquisition used to process spectroscopic measurements. The light coming from the plasma was analyzed by using a spectrometer of 1 m focal length equipped with a 2 400 groves/mm holographic grating. Intensity measurements were calibrated by using the system spectral response (carried out in a previous experiment) [45]. The spectral resolution was 0.004 nm and 0.01 nm when using the photomultiplier (OH and H_β records) and the CCD camera (Ar I spectra), respectively. The light was collected through 50 μm diameter optical fiber (UV-VIS high OH fiber with a range of transmission wavelength 200-800 nm). A UV-VIS collimating beam probe was coupled to the optical fiber giving a 0º-45º of field of view and 3mm of aperture. Thus, an Abel inversion [47] was precluded. Consequently, the values reported for the quantities measured side-on in this work should be considered to be average ones for a transversal section of the plasma column associated with a specific axial position, and the values obtained from end-on

measurements must be interpreted as average ones for the whole plasma column. As is habitual for SWD [18, 21], the axial origin of the measurement was assumed to coincide with the end of the column ($z = 0$).

5. Results and discussion

5.1. Temperatures and electron density

Figure 2 shows the axial variation of the electron temperature values estimated from line-to-continuum method. This profile was practically constant (~13 000 K) all along the plasma column and in good agreement with those predicted by the model of Nowakowska *et al*. [26]. It can also be noted that the values of T_e in neon SWDs are higher (~ 50 %) than those obtained for the argon columns [18, 21] under the same experimental condition of pressure and frequency, but lower than those theoretically predicted for helium SWDs [22]. The different ionization potential values for helium, neon and argon gases are responsible for the different electron temperature values found in the three kinds of SWD [29], and explain why the electron temperature in neon SWD has values between those of helium and argon discharges.

Figure 2 also represents the axial gas temperature profile obtained for the neon plasma column studied. This profile was also constant (~1 300 K) and comparable to those reported for a similar plasma generated using argon as a support gas, showing a good agreement with that calculated from the Nowakovska *et al.* [26] model.

It is shown that the electron temperature was much higher than that of gas ($T_e >> T_{gas}$) which indicates that the discharge is clearly a *2T* plasma, and also reflects the inefficient exchange of kinetic energy through the collisions between the electrons and heavy particles present in these neon discharges, due to their marked difference in mass.

Figure 3 shows the axial profiles of the electron density for the neon SWD studied in this work. For comparison purposes, the axial profile obtained for a tube of 1 mm inner diameter and the axial profiles obtained by Kabouzi *et al.* [24] for higher radius discharges (R = 2 and 3mm) in neon and helium SWD generated at atmospheric pressure and 2.45 GHz are also shown. Electron density profiles for argon SWDs studied by García et *al.* [21] created in quartz tubes of R = 0.5 mm have also been included. It can be seen that the electron density decreased towards the end of the discharge, as expected for a surface-wave sustained discharge [48]. The n_e axial profiles for neon plasma had values ranging between 1 and 2 × 10^{14} cm^{-3}; these values were lower than those obtained for argon SWDs (2.1- 5.5 × 10^{14} cm^{-3}) [21].

The electron density values found in neon SWD help to explain why the gas temperature has similar values in neon and argon SWDs. In the neon discharge higher values of T_{gas} could be expected than for argon, because of both the higher value of T_e and the smaller mass of the neon atoms, which increase the effectiveness of the energy transfer in electron-heavy particle interactions. But on the other hand, the electron density is lower in neon SWDs than in argon SWDs; thus, the number of collisions between electron and heavy particles (also determining the energy transfer) is lower, resulting in a similar transference of energy in neon and argon plasmas, and thus similar values of T_{gas}.

In Fig. 3, the difference in slope shown by the n_e axial profiles for each one of the three gases can be explained in terms of the direct relation of this slope to electron-atom collision frequency for the momentum transfer ν (characteristic parameter of the discharge that depends only on the pressure and gas temperature) and of the inverse dependence of the slope on the discharge tube radius [49]. In Fig. 4 electron-atom

collision frequency ν is represented for argon, neon and helium gases, normalized to microwave frequency, as a function of electron temperature. To compute ν, the following expression was used

$$\nu = \langle N \mathrm{v}_e Q \rangle \qquad (20)$$

where $\langle\ \rangle$ denotes integration over the Maxwellian electron energy distribution function, $N \approx n_1$ is the total density of neutral atoms, v_e is the velocity of the electrons, and Q is the momentum transfer cross section [50]. In this figure, it can be observed that in the interval of 5 000K $\leq T_e \leq$ 20 000K, the frequency for momentum transfer is much higher for helium plasmas than for neon and argon. On the other hand, the values of ν for argon and neon discharges are close, which explains the similar slopes dn_e/dz observed for both discharges in the same conditions of discharge radius.

From Fig. 4 it can also be inferred: 1) for argon plasmas at atmospheric pressure where ν/ω = 1.3-4.5 [51], $T_e \cong$ 7 000 K, which agrees with experimental results obtained by García *et al.* [21]; 2) for helium plasmas where ν/ω = 20 [52], the curve predicts a T_e ≅ 20 000 K, similar to those obtained for other helium MIPs at atmospheric pressure [40]; and 3) for neon plasmas, a value of ν/ω = 5 corresponds to the electron temperature ~13 000 K estimated using the line-to-continuum method, which agrees with the results of the Nonavoska *et al.* model [26].

5.2. Power absorbed per electron

The power absorbed per electron in the plasma (θ) necessary to preserve the discharge in a stationary state is usually employed to characterize and compare microwave plasmas [1, 18, 21]. This parameter expresses the balance between the power θ_L that the (average) electrons lose to the discharge (through various mechanisms) and the power θ_A that it absorbs from the microwave field to compensate for this loss.

The average θ_A value for the plasma columns is defined as being the ratio between the microwave power absorbed (P_{abs}) and the number of electrons (N_e) present in the discharge (calculated from the axial electron density profile Fig. 3) using the equation:

$$\theta_A = \frac{P_{abs}}{N_e} = \frac{P_{abs}}{\pi R^2 \int_0^l n_e dz} \qquad (21)$$

where R is the inner radius of the tube and l the plasma length. In our calculation, l was the length of the downstream column and P_{abs} was considered as 200 W (because the other 200 W were employed in the generation of the upstream column).

For the neon SWD studied, the value obtained was ≈ 5.2 pW, higher than those obtained for argon SWD columns (1.5-2.6 pW) [18, 21]. So maintaining an electron in the neon SWD is more expensive, from an energetic point of view, than in the argon one but much cheaper than in the case of helium SWD (27-35 pW) [29]. We estimated the error bar on θ_A (from n_e error) to be ± 20%.

For comparison purposes, Table 3 presents a summary of the parameter values of helium, neon and argon plasmas. These values also permit an understanding of the discussion on the electron temperature values carried out in previous sections.

5.3. Absolute population densities of NeI levels

The absolute population of NeI excited levels was measured at different z positions along the plasma column. The axial gradient of the absolute population of NeI excited levels was very slight and shows the same behavior as the axial gradient of the electron density. Fig. 5 shows similar (approx. linear) dependency on the electron density of the population of several atomic neon levels. This result, together with that obtained for the temperatures ($T_e >> T_{gas}$), indicates that the excitation kinetics in the discharge was controlled by the electrons. A similar result was found by Calzada *et al.* [18, 20] for the excited levels in a surface-wave argon column and flame, respectively.

Figure 5 also includes the densities of three argon atom excited levels with a similar ionization potential to what was obtained by García *et al.* [21]. This figure shows that the populations of the argon levels are higher than those of the neon levels, which is comprehensible when taking into account that the excitation of the atomic levels in argon plasmas is enhanced because of their higher electron density values.

As commented in Section 3, metastable Ne($^3P_0$) and resonant Ne($^3P_1$) levels were measured using a self absorbing method. This method has been used successfully by Santiago *et al.* [43, 44] in microwave argon plasmas at atmospheric pressure in capillary tubes. The a parameter necessary in the calculation was determined as described in Ref. 55. In the plasmas studied, the Lorentzian part of the line profiles corresponding to transitions with a quantum number $p < 6$ is mainly ascribed to the Van der Waals effect [56, 57]. Taking into account that the Van der Waals effect depends only on the gas temperature and this magnitude is constant throughout the discharge, the a parameter for the spectral lines used in this self-absorption method was considered to be approximately constant all along the plasma column. Table 4 shows the lines used in the

self-absorption method as well as the necessary parameters in Eq. (15). The curves of r versus $k_0 l$ for different values of k_{01}/k_{02}, a_1 and a_2 corresponding to each pair used in the $^3P_0$ and $^3P_1$ level population measurement, are drawn in Fig. 6 [43, 44].

To perform this determination the fact that SWDs at atmospheric pressure have similar characteristic parameters when studied from their end [18, 21] was used. The side-on and end-on measurements of light intensities in each z position were taken by changing the microwave power and, therefore, by generating different plasma columns of different lengths [55]. The population density values found for the first metastable state Ne($^3P_0$) and the first resonant one, Ne($^3P_1$), were 2.1×10^{11}cm^{-3} and 1.7×10^{11}cm^{-3}, respectively, not showing any axial variation along the plasma column.

5.4. Degree of thermodynamic equilibrium

Figure 7 shows the Boltzmann-plot of neon excited levels obtained at z = 4.5 cm axial position of the plasma column. The plot also includes the value corresponding to the ground state and metastable and resonant levels. The Saha distribution is also depicted in this ASDF representation, including the *Saha point* which corresponds to the population for the highest excited level obtained from Eq.(1) when E_{ip} is equal to zero.

The overpopulation of the excited states with respect to the Saha distribution shows the ionizing character of the neon SWDs studied. None of the measured atomic levels were in pLSE and the departure from the Saha equilibrium was very high, which precluded considering the excitation temperature obtained from the Boltzmann plot as the electron temperature. This behavior contrasts with the recombining character of argon SWDs at atmospheric pressure [18, 21], but it is similar to that found for helium microwave discharges at atmospheric pressure [29, 30].

In order to measure the equilibrium departure for the discharge, the values of b_1 were calculated (see Table 5). The b_1 values obtained were around 10^5, so this plasma cannot be considered to be close to LTE. The high overpopulation of the ground state induced a larger excitation from the first to the second excited state (metastable) resulting in an overpopulation at this level. This overpopulation again caused a larger excitation from second to third level, etc, and, consequently a stepwise ionisation flow was established in the atomic system. Jonkers *et al.* [29] have found a similar ionizing behavior in the helium microwave (2.45 GHz) torch generated using a *TIA* device [9], with radial dimensions of the same order (~ 1-2 mm). Table 5 also includes the b_1 values of a microwave-induced argon plasma at atmospheric pressure obtained by Calzada *et al.* [58]. It can be noted that the b_1 parameter in the argon plasma increases with z position while in the neon plasma it remains practically constant throughout the column. This fact, together with the slight axial variability of the electron density and temperatures in the neon SWD, permitted us to expect negligible axial changes in the discharge kinetics, which is in agreement with the slight variation in the NeI excited level populations shown in Fig.5.

The monotonic decrease in b_p as a function of principal quantum number p can be observed in Fig. 8. This behavior is also characteristic of the ionizing plasmas. The bottle-neck in this ionisation process is the relatively great step from the first (ground) to second (metastable) level [27, 29].

Margot [22] has calculated the b_1 parameter in surface-wave helium plasma at atmospheric pressure by means of a collisional-radiative model finding a value of about 2×10^6 for this parameter with $n_e = 3\times10^{13}$ cm^{-3} and T_{gas} = 2 000 K. In the case of helium, Margot has indicated that the great departure from the Saha equilibrium can be

explained by the existence of ionization routes that do not involve electrons (associative ionization) and by the fact that dissociative recombination of He_2^+ ions is a significant mechanism for electron losses. The importance of dissociative recombination to explain the equilibrium departure in atmospheric argon SWD has also been studied by Sáinz *et al.* [23]. The role of the dimmer ions Ne_2^+ in the excitation kinetics of the neon SWD at atmospheric pressure could also be expected to be important, although a collisional-radiative model of this neon discharge would be necessary to confirm this statement.

6. Conclusions

This paper presents the results of an experimental study of a surface-wave sustained neon plasma created and maintained at atmospheric pressure and frequency of 2.45 GHz. For this purpose, its characteristic parameters (temperatures, densities and power absorbed by electron) were measured by using emission spectroscopic techniques. A comparison with other noble gas SWDs (helium and argon) has been carried out. In the neon discharge studied, the gas temperature was axially constant at a value of about 1 300 K. The electron temperature estimated (from line-to-continuum method) was 13 000 K, and the values of electron density ranged between 1 and 2×10^{14} cm^{-3}. The value of θ parameter was 5.2 pW, higher than that obtained for argon SWDs, and lower than that corresponding to helium SWDs, obtained under similar experimental conditions. So maintaining an electron in the neon SWD is more expensive from an energetic point of view than in that of argon, but much cheaper than in the case of helium.

In the neon discharges studied, a great departure from the Saha equilibrium has been demonstrated, finding b_1 parameter values of about 10^5. The cause for this departure could be related to microscopic processes which involve neon molecular ions.

Aknowledgements

The authors wish to thank both the Spanish Dirección General de Investigación (Secretaría de Estado de Política Científica y Tecnológica) contracts Num. FTN2002-02595 and. ENE2005-00314 and the European community (FEDER founds) for their financial aid.

References

[1] *Microwave discharges: Fundamentals and Applications*, edited by C. M. Ferreira and M. Moisan, NATO ASI Series B, Vol. 302 (Plenum, New York, 1993)

[2] S. Moreau, M. Moisan, M. Tabrizian, J. Barbeau, J. Pelletier, A. Ricard, L. Yahia Using the flowing afterglow of a plasma to inactivate Bacillus subtilis spores: Influence of the operating conditions, J. Appl. Phys. 88 (2000) 1166-1174.

[3] Y. Kabouzi, M. Moisan, J.C. Rostaing, C. Trassy, D. Guerin, D. Keroack, Z. Zakrzewski, Abatement of perfluorinated compounds using microwave plasmas at atmospheric pressure, J. Appl. Phys. 93 (2003) 9483-9496.

[4] S. Ilías, C. Campillo, C.F.M. Borges, M. Moisan, Diamond coatings deposited on tool materials with a 915 MHz scaled up surface-wave-sustained plasma, Diamond and Relat. Mater. 9 (2000) 1120-1124.

[5] M. Moisan, Z. Zakrzewski, R. Pantel, P. Leprince, A waveguide-based launcher to sustain long plasma columns through the propagation of an electromagnetic surface-wave, IEEE Trans. Plasma Sci. 12 (1984) 203-214.

[6] M. Chaker, M. Moisan, Z. Zakrzewski, Microwave and rf surface-wave sustained discharges as plasma sources for plasma chemistry and plasma processing, Plasma Chem. and Plasma Process. 6 (1986) 79-96.

[7] M. Moisan, M. Chaker, Z. Zakrzewski, J. Paraszczak, The wave-guide surfatron - A high-power surface-wave launcher to sustain large-diameter dense-plasma columns, J. Phys. E 20 (1987) 1356-1361.

[8] G. Sauvé, M. Moisan, Z. Zakrzewski, Slotted wave-guide field applicator for the generation of long uniform plasmas, Journal of Microwave Power and Electromagnetic Energy 28 (1993) 123-131.

[9] A. Ricard, L. St-Onge, H. Malvos, A. Gicquel, J. Hubert, and M. Moisan, Microwave-excited plasma torch - 2 complementary configurations, J. Phys. III 5 (1995) 1269-1285.

[10] M. Moisan, Z. Zakrzewski, R. Grenier, G. Sauvé, Large-diameter plasma generation using a wave-guide-based field applicator at 2.45-GHz, Journal of Microwave Power and Electromagnetic Energy 30 (1995) 58-65.

[11] G. Sauvé, M. Moisan, Z. Zakrzewski, C.A. Bishop, Sustaining long linear uniform plasmas with microwaves using a leaky-wave (troughguide) field applicator, IEEE Trans. Antennas and Propagation 43 (1995) 248-256.

[12] Z. Zakrzewski , M. Moisan, Plasma sources using long linear microwave field applicators - main features, classification and modelling, Plasma Sources Sci. and Techn. 4 (1995) 379-397.

[13] M. Moisan, R. Grenier, Z. Zakrzewski, The electromagnetic performance of a surfatron-based coaxial microwave plasma torch, Spectrochim. Acta B 50 (1995) 781-789.

[14] M. Moisan, Z. Zakrzewski, and J.C. Rostaing, Waveguide-based single and multiple nozzle plasma torches: the TIAGO concept, Plasma Sources Sci. and Techn. 10 (2001) 387-394.

[15] Z. Zakrzewski, M. Moisan, Linear field applicators, J. Phys. IV 8 (P7) (1998) 109-118.

[16] J. Pollak, M. Moisan, Z. Zakrzewski, Long and uniform plasma columns generated by linear field-applicators based on stripline technology, Plasma Sources Sci. and Techn. 16 (2007) 310-323.

[17] T. Fleish, Y. Kabouzi, M. Moisan, J. Pollak, Castaños-Martínez, H. Nowakowska, Z. Zakrzewski, Designing an efficient microwave-plasma source, independent of operating conditions, at atmospheric pressure, Plasma Sources Sci. and Techn. 16 (2007) 173-182.

[18] M. D. Calzada, M. Moisan, A. Gamero, and A. Sola, Experimental investigation and characterization of the departure from local thermodynamic equilibrium along a surface-wave-sustained discharge at atmospheric pressure, J. Appl. Phys. 80 (1996) 46-55.

[19] M. D. Calzada, M. Sáez, and M. C. García, Characterization and study of the thermodynamic equilibrium departure of an argon plasma flame produced by a surface-wave sustained discharge, J. Appl. Phys. 88 (2000) 34-39.

[20] M. D. Calzada, M. C. García, J. M. Luque, and I. Santiago, Influence of the thermodynamic equilibrium state in the excitation of samples by a plasma at atmospheric pressure, J. Appl. Phys. 92 (2002) 2269-2275.

[21] M. C. García, A. Rodero, A. Sola, A. Gamero, Spectroscopic study of a stationary surface-wave sustained argon plasma column at atmospheric pressure, Spectrochim. Acta B 55 (2000) 1733-1745.

[22] J. Margot, Studies of emission spectra in helium plasmas at atmospheric pressure and local thermodynamical equilibrium, Phys. Plasmas 8 (2001) 2525-2531.

[23] A. Sáinz, J. Margot, M.C. García, M.D. Calzada, Role of dissociative recombination in the excitation kinetics of an argon microwave plasma at atmospheric pressure, J. Appl. Phys. 97 (2005) No.113305.

[24] Y. Kabouzi, M. D. Calzada, M. Moisan, K. C. Tran, C. Trassy, Radial contraction of microwave-sustained plasma columns at atmospheric pressure, J. Appl. Phys. 91 (2002)1008-1019.

[25] Y. Kabouzi and M. Moisan, Pulsed microwave discharges sustained at atmospheric pressure: study of the contraction and filamentation phenomena, IEEE Trans. Plasma Science, 33 (2005), 292-293.

[26] Nowakowska, M. Jasinski, J. Mizeraczyk, Z. Zarkrzewski, Y. Kabouzi, E. Castaños-Martínez, M. Moisan, Surface-wave sustained discharge in neon at atmospheric pressure: model and experimental verification, Czech. J. Phys. 56 (2006) B964-B970.

[27] J. A. M. van der Mullen, Excitation equilibria in plasmas - a classification, Phys. Rep.-Rev. Sect of Physics Letters 191 (1990) 109-220.

[28] J. A. M. van der Mullen, D. A. Benoy, F. H. A. G. Fey, B. van der Sidje, J. Vlček, Saha equation for 2-temperature plasmas - theories, experimental-evidence, and interpretation, Phys. Rev. E 50 (1994) 3925-3934.

[29] J. Jonkers, H.P.C. Vos, J.A.M. van der Müllen, E.A.H. Timmermans, On the atomic state densities of plasmas produced by the "Torche a Injection Axiale", Spectrochim. Acta B 51 (1996) 457-465.

[30] A. Rodero, M.C. García, M.C. Quintero, A. Sola, A. Gamero, An experimental study of the deviation from equilibrium in a high-pressure microwave helium plasma produced by an axial injection torch, J. Phys. D 29 (1996) 681-686.

[31] H. Kafrouni, S. Vacquié, J.Phys D: Appl. Phys. 10 (1997), 1607-1616.

[32] T. Fujimoto, R. W. McWhriter, Validity criteria for local thermodynamic-equilibrium in plasma spectroscopy, Phys. Rev. A 42 (1990) 6588-6601.

[33] T. Fujimoto, Kinetics of ionization-recombination of a plasma and population-density of excited ions .2. Ionizing plasma, J. Phys. Soc. Jap. 47 (1979) 273-281.

[34] *Spectral Line Broadening by Plasmas*, H. R. Griem, New York: Academic, 1974.

[35] M. A. Gigosos, V. Cardeñoso, New plasma diagnosis tables of hydrogen Stark broadening including ion dynamics, J. Phys. B 29 (1996) 4795-4838.

[36] M. A. Gigosos, M.A. González and V. Cardeñoso, Computer simulated Balmer-alpha, -beta and -gamma Stark line profiles for non-equilibrium plasmas diagnostics, Spectrochim. Acta B 58 (2003) 1489-1504.

[37] J.M. Mermet, Inductively Coupled Plasma Emission Spectrometry, Part II: Applications and Fundamentals. P.W.J.M. Bowmans (Eds.) Wiley-Interscience. New York, 1987.

[38] G. J. Bastiaans, R.A. Mangold, The calculation of electron-density and temperature in Ar spectroscopic plasmas from continuum and line spectra, Spectrochim. Acta B 40 (1985) 885-892.

[39] A. Sola, M.D. Calzada and A. Gamero, On the use of the line-to-continuum intensity ratio for determining the electron-temperature in a high-pressure argon surface-microwave discharge, J. Phys. D. 28 (1995) 1099-1110.

[40] J. Jonkers, J.M. Regt, J.A.M. van der Mullen, H.P.C. Vos, F.P.J. de Groote, E.A.H. Timmermans, On the electron temperatures and densities in plasmas produced by the "Torche a Injection Axiale", Spectrochim. Acta B 51 (1996) 1385-1392**.**

[41] J. D. Yan, C. F. Pau, S. R. Wylie, and M. T. C. Fang, Experimental characterization of an atmospheric argon plasma jet generated by an 896 MHz microwave system, J. Phys. D: Appl. Phys. 35 (2002). 2594-2604.

[42] J. Jolly, M. Touzeau, Measurement of metastable-state densities by self-absorption technique, J. Quant. Radiat. Transfer. 15 (1975) 863-872.

[43] I. Santiago, M. Christova, M. C. García, M. D. Calzada, Self-absorbing method to measure the population of the metastable levels in an argon microwave plasma at atmospheric pressure, Eur. Phys. J. Appl. Phys. 28 (2004) 325-330.

[44] I. Santiago, M.D. Calzada, Population measurement of the 3p(5)4s configuration levels in an argon microwave plasma at atmospheric pressure, Appl. Spectrosc. 61 (2007) 725-733.

[45] C. Yubero, M.C. García and M.D. Calzada, Using halogen lamp to calibrate an optical system of UV-VIS radiation, Optica Applicata 38 (2008) (accepted for publication).

[46] J. Reader, C.H. Corliss, W.L. Wiese and G.A. Martin, Wavelenghts and Transition Probabilities for Atoms and Atomic Ions, NSRDS-NBS 68 (1980), Whasington D.C.

[46] A. Sáinz, A. Díaz, D. Casas, M. Pineda, F. Cubillo, M.D. Calzada, Abel inversion applied to a small set of emission data from a microwave plasma, Appl. Spectrosc. 60 (2006) 229-236.

[47] *Microwave Excited Plasmas*, edited by M. Moisan and J. Pelletier, Elsevier, New York, 1992.

[48] A. Granier, C. Boisse-Laporte, P. Leprince, J. Marec, P. Nghiem, Wave-propagation and diagnostics in argon surface-wave discharges up to 100-torr, J. Phys. D 20 (1987) 204-209.

[49] A. G. Robertson, Momentum-transfer cross-section for low-energy electrons in neon, J. Phys. B 5 (1972) 648-&.

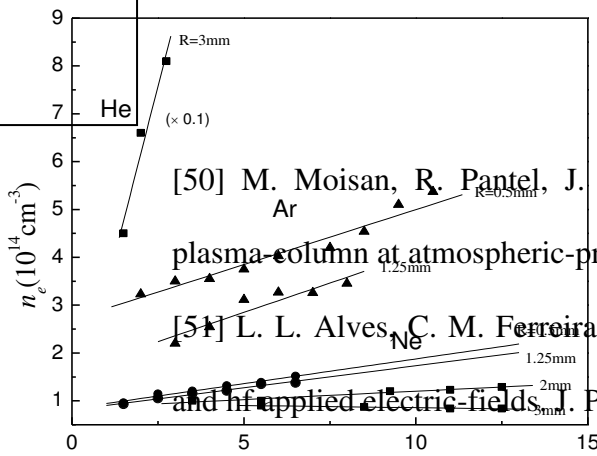

[50] M. Moisan, R. Pantel, J. Hubert, Propagation of a surface-wave sustaining a plasma-column at atmospheric-pressure, Contrib. Plasma Phys. 30 (1990) 293-314.

[51] L. L. Alves, C. M. Ferreira, Electron kinetics in weakly ionized helium under dc and hf applied electric-fields, J. Phys. D 24 (1991) 581-592.

[52] A. Pérès, L. L. Alves, J. Margot, T. Sadi, C. M. Ferreira, K. C. Tran, and J. Hubert, Plasma Chem. Plasma Process. **19**, 467 (1999).

[53] K. C. Tran, M. Sc. Thesis, Université de Montréal (1995).

[54] I. Santiago, M.C. García, M.D. Calzada, Experimental method for determining the damping parameter of spectral lines emitted by a microwave plasma at atmospheric pressure Appl. Spectrosc. 59 (2005) 1457-1464.

[55] A. Sáinz, M.D. Calzada and M.C. García, Mem.S.A.It 7, 232 (2005).

[56] M. Christova, E. Castaños-Martínez, M.D. Calzada, Y. Kabouzi, J.M. Luque and M. Moisan, Electron density and gas temperature from line broadening in an argon surface-wave-sustained discharge at atmospheric pressure, App. Spectrosc. 58 (2004)1032-1037.

[57] M. D. Calzada, A. Rodero, A. Sola, A. Gamero, Excitation kinetic in an Argon plasma column produced by a surface wave at atmospheric pressure, J. Phys. Soc. Jpn. 65 (1996) 948-954.

FIGURE CAPTIONS

Fig.1. Schematic diagram of the experimental set-up.

Fig.2. Gas and electron temperatures as a function of axial position along the neon plasma column.

Fig. 3. Electron density axial profiles measured in the present work for neon SWD columns (●). Axial profiles of electron density for other (neon and helium) SWD columns (■) [24] and argon SWD columns (▲) [21].

Fig. 4. Electron-atom collision frequency in helium, argon and neon plasmas at atmospheric pressure as a function of the electron temperature.

Fig. 5. Population density of several excited levels of NeI and ArI with a different ionization potential as a function of electron density

Fig. 6. Ratio *r* of intensities as a function of the absorption parameter for different pairs of spectral lines.

Fig. 7. The Boltzmann-plot of the absolute population density of NeI excited levels at z = 4.5 cm. The Saha distribution and the point corresponding to the ionization level (□) have also been plotted.

Fig. 8. Experimental *b(p)* parameter for the levels measured.

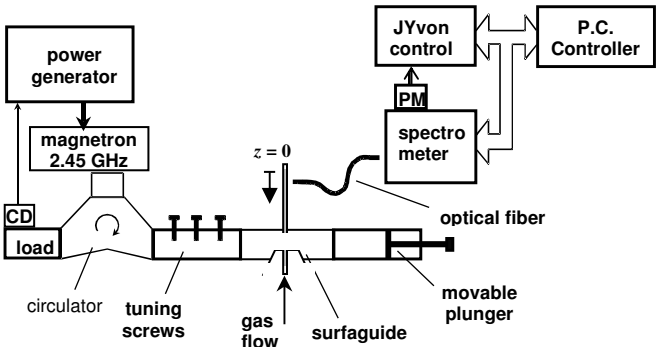

Fig. 1. Sáinz *et al.*

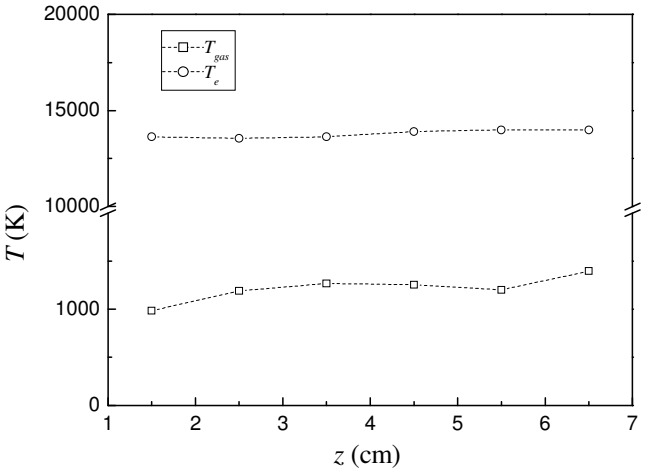

Fig. 2. Sáinz *et al.*

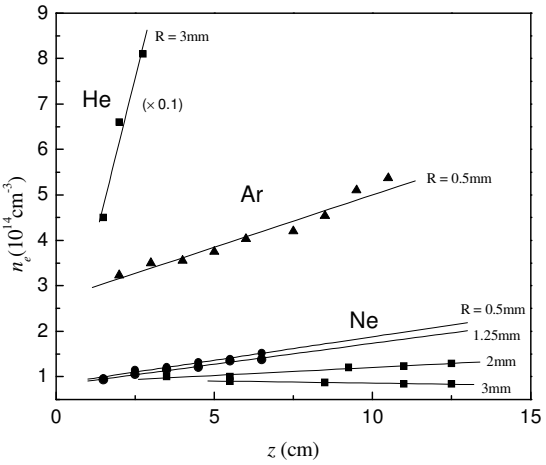

Fig. 3. Sáinz *et al.*

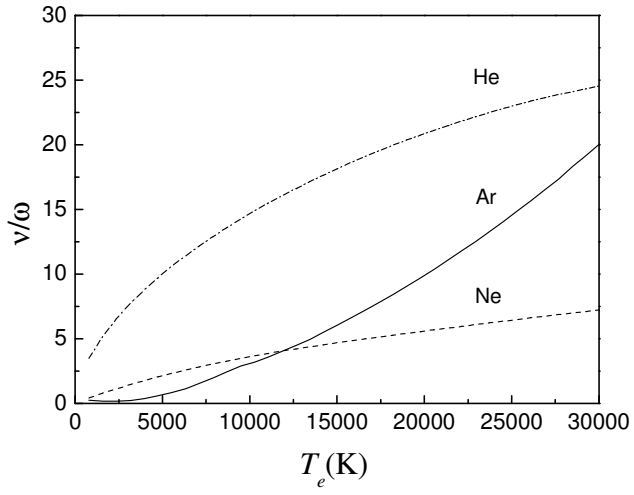

Fig. 4. Sáinz *et al.*

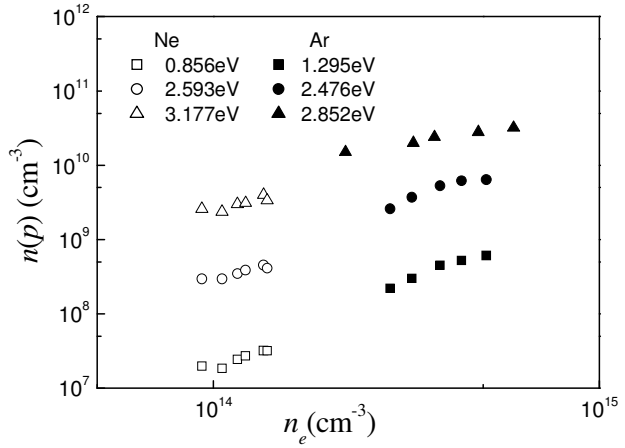

Fig. 5. Sáinz *et al.*

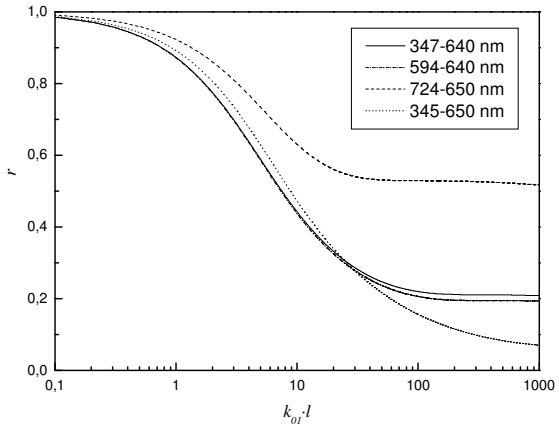

Fig. 6. Sáinz *et al.*

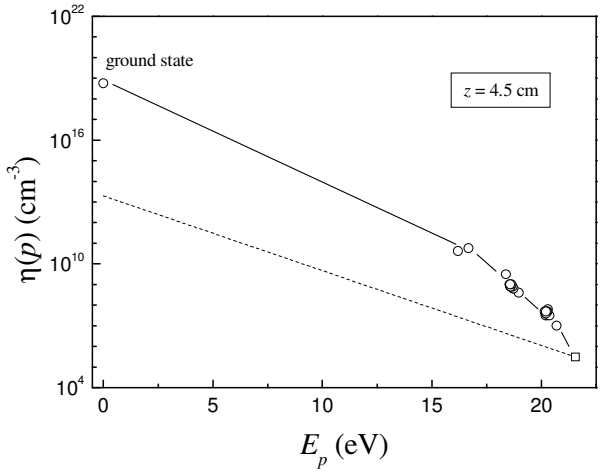

Fig. 7. Sáinz *et al.*

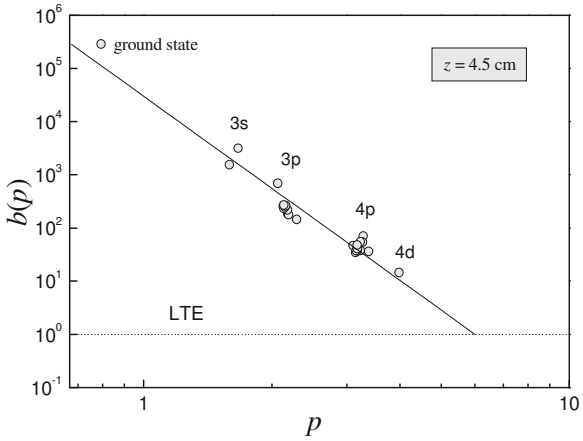

Fig. 8. Sáinz *et al.*

TABLE CAPTIONS

Table 1. Characteristic parameters for the Q_1 branch of the OH (0-0) band [34].

Table 2. Spectral line parameters for NeI levels used in this study [46].

Table 3. Values of the characteristic parameters in microwave helium, neon and argon plasmas generated at atmospheric pressure. [a]Ref. 53, [b]This work, [c]Refs. 18 and 23, [d]Ref. 54, [e]Ref. 51.

Table 4. Parameters of the spectral lines of NeI system used to measure the metastable and resonant populations.

Table 5. Values of the b_1 parameter at different positions along the plasma column for argon and neon plasmas.

λ (nm)	$A_{J'J''}$ (10^9 s^{-1})	K''	E_p (eV)
307.84	1.00	1	4.0252
307.99	1.70	2	4.0336
308.33	3.37	4	4.0629
308.52	4.42	5	4.0838
308.73	5.06	6	4.1089
309.24	6.75	8	4.1711
309.53	7.58	9	4.2083
309.86	8.41	10	4.2493

Table 1. Sáinz *et al.*

λ (nm)	E_p (eV)	g_p	A_{pq} (10^8 s^{-1})	Transition
345.41	20.25918	1	0.037	4p-3s
347.25	20.18844	7	0.017	4p-3s
350.12	20.21099	3	0.012	4p-3s
351.07	20.14965	3	0.0022	4p-3s
351.51	20.19692	5	0.0069	4p-3s
352.04	20.36886	1	0.093	4p-3s
359.35	20.29728	5	0.0099	4p-3s
360.01	20.29092	3	0.0043	4p-3s
363.36	20.25918	1	0.011	4p-3s
368.22	20.21418	5	0.0016	4p-3s
368.57	20.21099	3	0.0039	4p-3s
534.10	20.70231	3	0.11	4d-3p
585.24	18.96596	1	0.682	3p-3s
594.48	18.70407	5	0.113	3p-3s
602.99	18.72638	3	0.0561	3p-3s
626.64	18.69336	3	0.249	3p-3s
640.22	18.55511	7	0.514	3p-3s
650.65	18.57584	5	0.3	3p-3s
653.28	18.61271	3	0.108	3p-3s
692.94	18.63679	5	0.209	3p-3s
717.39	18.57584	5	0.0287	3p-3s
724.51	18.38162	3	0.0935	3p-3s
743.88	18.38162	3	0.0231	3p-3s

Table 2. Sáinz *et al.*

Gas	n_e ($\times 10^{14}$ cm^{-3})	T_g (K)	T_e (K)	ν / ω	θ (pW)
He	0.1	1 100-2 000[a]	20 000[d]	20[e]	27-35[a]
Ne	1-2	1 200[b]	13 000[b]	5[b]	5.2[b]
Ar	2.1-5.5	1 500[c]	7 000[c]	1.3-4.5[e]	1.5-2.6[c]

Table 3. Sáinz *et al.*

λ (nm)	Transition	f_{pq}	a
347.25	4p-3s($^3P_2$)	0.0043	0.75
594.48	3p-3s($^3P_2$)	0.0599	0.68
640.22	3p-3s($^3P_2$)	0.373	0.70
725.51	3p-3s($^3P_1$)	0.0736	0.88
345.42	4p-3s($^3P_1$)	0.0022	0.65
650.65	3p-3s($^3P_1$)	0.318	1.0

Table 4. Sáinz *et al*.

Gas	z (cm)	T_{gas} (K)	n_1 (cm^{-3})	n_1^S (cm^{-3})	b_1
Ne	2.5	1200	6.0×10^{18}	2.5×10^{13}	2.4×10^{5}
	4.5	1200	6.0×10^{18}	1.9×10^{13}	3.2×10^{5}
	6.5	1200	6.0×10^{18}	3.1×10^{13}	1.9×10^{5}
Ar	2	1400	5.3×10^{18}	4.0×10^{25}	1×10^{-7}
	4	1400	5.3×10^{18}	6.0×10^{23}	9.0×10^{-6}
	8	1400	5.3×10^{18}	1.0×10^{21}	5.0×10^{-3}

Table 5. Sáinz *et al.*